

## Article

# Ecological Environment Evaluation Based on Remote Sensing Ecological Index: A Case Study in East China over the Past 20 Years

Shangxiao Wang <sup>1,\*</sup> , Ming Zhang <sup>1</sup> and Xi Xi <sup>2</sup> <sup>1</sup> Nanjing Center of Geological Survey, China Geological Survey, Nanjing 210016, China<sup>2</sup> Institute of Geology, China Earthquake Administration, Beijing 100029, China

\* Correspondence: wangshangxiao@mail.cgs.gov.cn; Tel.: +86-025-84607905

**Abstract:** East China is one of the most active regions in terms of economic and social development, and with the accelerated urbanization process, environmental problems are becoming increasingly prominent. The objective, quantitative, and timely evaluation of spatial and temporal changes in ecological quality is of great significance for environmental protection and decision making. The remote sensing ecological index (RSEI) is an objective, fast, and easy ecological quality monitoring and evaluation technique which has been widely used in the field of ecological research, but it often involves problems of cloud occlusion and stitching difficulties when used to conduct large-scale and long-term monitoring. In this paper, based on the Google Earth Engine (GEE) platform, an RSEI was constructed using MODIS data products to evaluate the spatial and temporal changes in ecological quality in East China over the past 20 years. The study shows the following: (1) The mean RSEI values in 2000, 2005, 2010, 2015, and 2020 were 0.67, 0.55, 0.59, 0.58, and 0.63, respectively, with the mean values first decreasing and then showing a stable increasing trend. In Shanghai and Jiangsu, the mean RSEI values show a fluctuating characteristic of “falling and then rising”, and large respective decreases of 32.4% and 25.8% throughout the monitoring period. The RSEI values in Fujian Province showed a relatively stable upward trend during the study period (19% increase). (2) The RSEI spatially correlated clustering maps of the local indicators showed that the regions with a high degree of clustering are mainly located in Quzhou City, Zhejiang Province, Ningde City, Fujian Province, and northern Anhui Province (Bozhou and Huabei). With the promotion of ecological civilization and the enhancement of environmental protection awareness, the vegetation cover has significantly increased, which has led to the rise in RSEI values. The low values are mainly distributed in densely populated areas with more human activity, such as the central-eastern part of Jiangsu Province, central Anhui Province, Shanghai, and northern Zhejiang Province. With the development of cities, impervious surfaces occupy more and more ecological land, which eventually affects the regional RSEI values. (3) This research provides a promising method for the evaluation of spatial and temporal changes in ecological environment quality based on an RSEI and GEE. The image processing, based on GEE cloud computing, can help overcome the problems of missing remote sensing data, chromatic aberrations, and spatial and temporal inconsistency, which could greatly improve the efficiency of image processing and extend the application of the remote sensing ecological index to large-scale, long-term ecological monitoring. The research results can provide a reference for improving the applicability and accuracy of remote sensing ecological indices and provide a theoretical basis for ecological conservation and land management in the context of rapid urbanization.



**Citation:** Wang, S.; Zhang, M.; Xi, X. Ecological Environment Evaluation Based on Remote Sensing Ecological Index: A Case Study in East China over the Past 20 Years. *Sustainability* **2022**, *14*, 15771. <https://doi.org/10.3390/su142315771>

Academic Editor: Antonio Miguel Martínez-Graña

Received: 31 October 2022

Accepted: 24 November 2022

Published: 27 November 2022

**Publisher's Note:** MDPI stays neutral with regard to jurisdictional claims in published maps and institutional affiliations.



**Copyright:** © 2022 by the authors. Licensee MDPI, Basel, Switzerland. This article is an open access article distributed under the terms and conditions of the Creative Commons Attribution (CC BY) license (<https://creativecommons.org/licenses/by/4.0/>).

**Keywords:** RSEI; ecological environment quality; Google Earth Engine; change in land use

## 1. Introduction

Human activity has caused considerable damage to ecosystems worldwide and have attracted widespread attention [1]. In recent years, the rapid development of East China

has made it necessary to monitor ecological changes over many years. Remote sensing has been widely used in the ecological environment field, with its advantages of fast, real-time, and large-scale monitoring [2]. Additionally, some remote sensing-based indices have been used to describe the status of the ecological environment, such as the normalized vegetation index (NDVI), which is widely used in many ecological studies [3–6]. The leaf area index (LAI) is another commonly used vegetation index for monitoring and analyzing environmental changes [7,8]. The enhanced vegetation index (EVI) is commonly used to reflect changes in vegetation cover in ecological environments [9–12]. However, most of these remote sensing-based ecological assessments are based on a single index, and it is not sufficient to use only one ecological indicator to evaluate the state of an ecosystem due to the complexity and diversity of influencing factors [13,14]. The remote sensing ecological index (RSEI) is used for the rapid monitoring and evaluation of the ecological status of cities using natural factors and based entirely on remote sensing technology, and it brings new hope regarding the realization of a large-scale and long-term ecological evaluation method [1,15]. The RSEI overcomes the shortcomings of a single indicator, makes the aggregation of sub-indicators more reasonable, and has been successfully applied to several regions to support the analysis, modeling, and prediction of regional ecological characteristics [16–18]. It was found that the model is visualizable, scalable, and comparable at different spatial and temporal scales, and its reliability and credibility have been verified in previous studies [19–22]. However, the construction process of an RSEI is complex and time-consuming when using traditional professional remote sensing software to evaluate long-term changes in ecological quality at large scales. As an open access and free platform for research, education, and non-profit purposes, Google Earth Engine (GEE) has been widely used, especially for research at large scales, such as the global scale [23–25]. Users can compute resources and process them directly on the platform, and some datasets, such as the Landsat and Modis series, have been preprocessed to convert the raw numbers to top-of-atmosphere reflectance or even surface reflectance, making them suitable for further analysis without the need for specialized software for radiometric and atmospheric correction [26]. As a region with one of the highest levels of economic development in China, the continuous urbanization process in East China has caused dramatic changes in the natural ecological environment of China's coastal areas. In 2020, the urbanization rates of Jiangsu, Zhejiang, and Shanghai all exceeded 70%, bringing a series of environmental problems. In 2006, Fujian Province became the first national ecological civilization demonstration area in China, with special emphasis placed on environmental protection and sustainable development, including the development and protection of land space, environmental governance systems, water resources, and comprehensive improvement measures for the water environment. At present, Fujian Province ranks first in the country in terms of forest coverage and ecological environment index, and the ecological environment has been greatly improved [27,28]. Using the premise of ensuring the sustainable development of the region, it is important to study the interactions between the ecological environment and human activity in recent decades. Therefore, based on multi-source remote sensing data, this paper explores the interaction between changes in ecological environment and the urbanization process in East China. The specific objectives of this study were to (1) monitor the long-term (2000–2020) dynamic changes in the ecological environment in East China in the context of rapid urbanization based on Google Earth Engine (GEE) and (2) evaluate the relationship between the ecological environment and land use/cover in East China over the past 20 years and recognize the impact of continuous land-use changes on the local environment.

## 2. Materials and Methods

### 2.1. Study Area

East China is close to the eastern coast of China (Figure 1), is rich in material resources, has well-developed commodity production, has a full range of industrial sectors, produces a high degree of work in ecological surveys, and is the economic zone with the highest level

of comprehensive technology in China [29]. The northern part is the North China Plain, the central part is the Yangtze River Delta Plain, and the southern part is mountainous. The Yangtze River Delta city cluster in East China is a city clusters with one of the highest urban density and urbanization levels in China. It consists of 14 prosperous cities in Shanghai, Jiangsu, and Zhejiang, and includes four urban agglomerations, namely Nanjing–Zhenjiang–Yangzhou, Suzhou–Wuxi–Changzhou, Shanghai, and Hangzhou Bay [30]. East China is located in the East Asian monsoon region in the lower delta of the Yangtze River. According to the distribution of annual precipitation, the precipitation in East China is greater in the south than in the north, while there is more in the east and less in the west. Fujian and Jiangxi on the southeast coast have the most abundant rainfall, with annual precipitation above 1600 mm, while the annual precipitation in Zhejiang and Hunan is about 1500 mm [31].

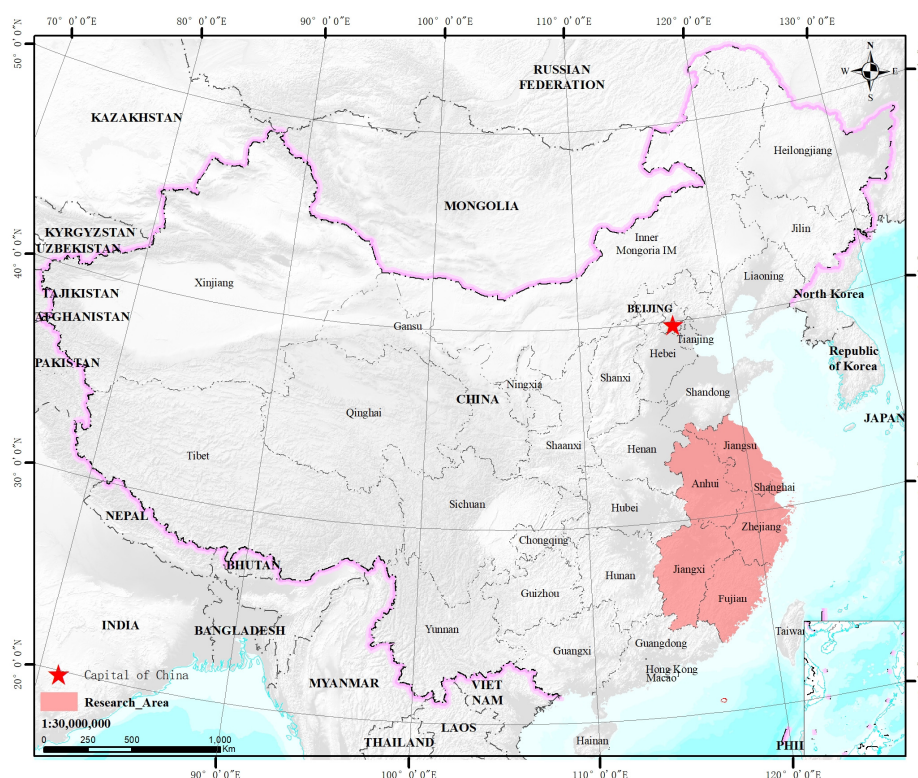


**Figure 1.** Map showing location of East China.

## 2.2. Data Source and Pre-Processing

### 2.2.1. Land-Use Data

The GLC\_FCS30 product was used for land-use data. The newly developed global 30 m fine land-cover classification product for 2020 (GLC\_FCS30-2020) was used for the baseline data, and a long-term series land-cover dynamic monitoring scheme combining coupled change detection and dynamic update was proposed, using all Landsat satellite data from 1984 to 2020 (Landsat TM, ETM+ and OLI) for the period 1985–2020 to produce a global 30 m fine surface-cover dynamic monitoring product. A total of 29 ground cover types were included, and the update cycle was 5 years [32,33].

### 2.2.2. Image Data

#### 1. High-resolution images

High-resolution remote sensing image data were mainly obtained through the GF-1 and GF-2 data acquired by the Geological Cloud Platform (<http://geocloud.cgs.gov.cn> accessed on 1 March 2020). High-resolution images were mainly used for the analysis of the RSEI evaluation results.

## 2. MODIS images

The construction of the RSEI involved four ecological components, namely, greenness, humidity, heat, and dryness. The NASA Land Processes Distributed Active Archive Center (LPDAAC) Collections under USCS provides standard data products for different application scenarios based on Level 1B data. The standard data products include Land Surface Reflectance, Land Surface Temp and Emiss, and Vegetation Indices. The greenness component was extracted from the MOD13A1 V6 image set in the Vegetation Indices product. This image provides vegetation indices (VI) for each pixel location at a spatial resolution of 500 m and was synthesized using the best pixels over a 16-day period. The thermal component was extracted from the MOD11A2 V6 image set in the Land Surface Temp and Emiss product, which provides an 8-day average land surface temperature at a spatial resolution of 1 km [34]. In addition, the product removes cloud-contaminated pixels from the Level 2 and Level 3 surface temperature products to improve data quality. The humidity and dryness components were derived from the MOD09A1 image set in the Land Surface Reflectance product. MOD09A1 V6 images provide surface spectral reflectance estimates in Tera MODIS bands from 1 to 7, corrected for atmospheric bars (e.g., gas, aerosol amine, and Rayleigh scattering) and, for each pixel, the product performs pixel compositing over an 8-day cycle.

### 2.3. Construction of Remote Sensing Ecological Index

The RSEI consists of a Normalized Vegetation Index (NDVI), Humidity Component (WET), Land Surface Temperature (LST), and Dryness Index (NDBSI), which, respectively, reflect the four ecological components of greenness, humidity, heat, and dryness that are closely related to human survival (Figure 2).

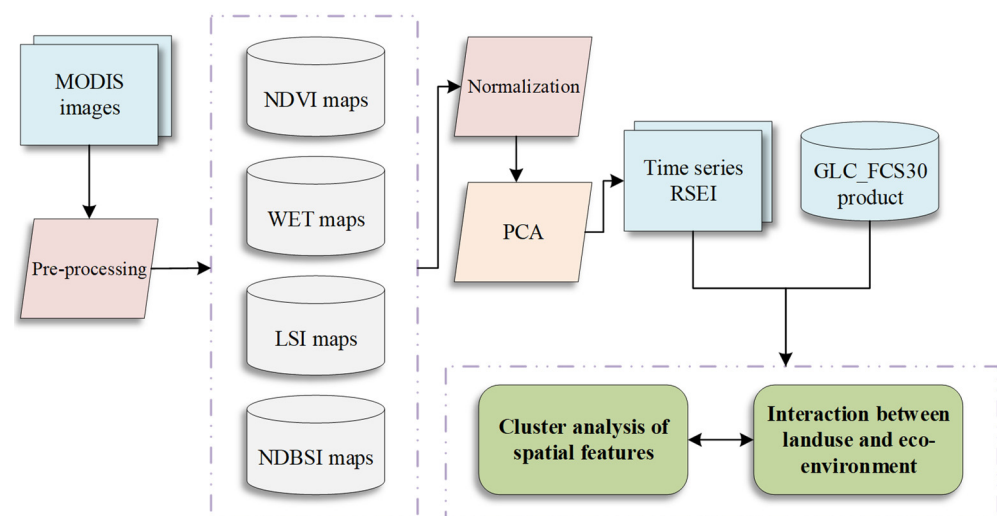


**Figure 2.** Map of technical routes and workflow for calculating and analyzing.

#### 2.3.1. NDVI

The NDVI was constructed according to the absorption and reflection characteristics of vegetation foliage in the red band and near-infrared band, which can reflect the plant biomass, leaf area index, and vegetation cover. Therefore, the NDVI was used to characterize the urban greenness index, and the calculation method is shown in Equation (1).

$$NDVI = \frac{\rho_{NIR} - \rho_{red}}{\rho_{NIR} + \rho_{red}} \quad (1)$$

where  $\rho_{red}$  and  $\rho_{NIR}$  denote the reflectance of the red and near-infrared bands corresponding to the image, respectively. Since the MOD13A1 V6 contains the NDVI layer, it is not

necessary to calculate this according to the formula and use these data directly as the greenness component.

### 2.3.2. WET

The humidity component (*wet*) based on the tassell cap transformation can reflect the surface water body conditions, especially the moisture state of the soil, and the calculation method is shown in Equation (2).

$$wet = a_1\rho_{red} + a_2\rho_{NIR1} + a_3\rho_{blue} + a_4\rho_{green} + a_5\rho_{NIR2} + a_6\rho_{SWIR1} + a_7\rho_{SWIR2} \quad (2)$$

where  $\rho_{red}$ ,  $\rho_{NIR1}$ ,  $\rho_{blue}$ ,  $\rho_{green}$ ,  $\rho_{NIR2}$ ,  $\rho_{SWIR1}$  and  $\rho_{SWIR2}$  represent the reflectance of the 7 bands in the MOD09A1 images. For the MODIS images, the coefficients of  $a_1$  to  $a_7$  are 0.11471, 0.24892, 0.24083, 0.31324,  $-0.31225$ ,  $-0.64166$ , and  $-0.5087$ , respectively [35].

### 2.3.3. LST

Unlike Landsat images for small-scale surface temperature inversion, Modis thermal infrared images with a high temporal resolution (8 days) and moderate spatial resolution (1 km) have become an indispensable data source for large-scale regional surface temperature inversion. The thermal component was derived from the DLST layer of the MOD11A2 V6 Dataset.

### 2.3.4. NDBSI

Buildings are an important part of the urban artificial ecosystem, and the impervious surfaces of buildings have replaced the original natural ecosystem, which has led to the "dryness" of the ground surface. Therefore, the building bare soil index was used to represent the "dryness" [17]. The index-based built-up index (*IBI*) and bare soil index (*SI*) were used to synthesize the dryness index, the result of which is called the normalized difference built-up and soil index (*NDBSI*) and is calculated as follows:

$$NDBSI = (SI + IBI)/2 \quad (3)$$

$$SI = \frac{(\rho_{SWIR1} + \rho_{red}) - (\rho_{NIR1} + \rho_{blue})}{(\rho_{SWIR1} + \rho_{red}) + (\rho_{NIR1} + \rho_{blue})} \quad (4)$$

$$IBI = \frac{2\rho_{SWIR1}/(\rho_{SWIR1} + \rho_{NIR1}) - [\rho_{NIR1}/(\rho_{NIR1} + \rho_{red}) + \rho_{green}/(\rho_{SWIR1} + \rho_{green})]}{2\rho_{SWIR1}/(\rho_{SWIR1} + \rho_{NIR1}) + [\rho_{NIR1}/(\rho_{NIR1} + \rho_{red}) + \rho_{green}/(\rho_{SWIR1} + \rho_{green})]} \quad (5)$$

where  $\rho_{red}$ ,  $\rho_{NIR1}$ ,  $\rho_{blue}$ ,  $\rho_{green}$  and  $\rho_{SWIR1}$  represent the reflectance of the 5 bands in the MOD09A1 images.

After calculating the four ecological components based on the MODIS data, a principal components analysis (PCA) was used to synthesize the multiple indicators to avoid the bias of subjective human factors in the weight-setting process. Since the above four components are not uniform in scale, the above indicators had to be regularized. Following this, the PCA was performed and the first principal component (PC1) was used to construct the RSEI.

## 2.4. Cluster Analysis

Cluster analysis enables the spatial clustering of elements with high or low values and can identify hot and cold spots with statistical significance. The calculation method is shown below [36]:

$$I_i = \frac{x_i - \bar{X}}{S_i^2} \sum_{j=1, j \neq i}^n w_{ij}(x_j - \bar{X}) \quad (6)$$

where  $I_i$  is local Moran's  $I$  value,  $x_i$  is the attribute of element  $i$ ,  $\bar{X}$  is the mean of the corresponding attributes,  $w_{ij}$  is the spatial weight between elements  $i$  and  $j$ , and

$$S_i^2 = \frac{\sum_{j=1, j \neq i}^n (x_j - \bar{X})^2}{n - 1} \quad (7)$$

where  $n$  is equal to the number of elements.

A positive value of  $I$  indicates that the element has neighboring elements that contain equally high or equally low attribute values. A negative value of  $I$  indicates that the element has neighboring elements that contain different values, and the element is an outlier. The final results are classified as statistically significant high-value (HH) clusters and low-value (LL) clusters; high values are mainly surrounded by low values (HL) and low values are mainly surrounded by high values (LH).

### 2.5. Google Earth Engine

GEE is a cloud-based platform for planetary-level geospatial analysis that enables Google's enormous computing power to address a variety of high-impact social and environmental issues [37]. GEE hosts several petabytes of spatial data in the cloud, including the Landsat series, the MODIS series, the Sentinel series, and more, with more than 6000 scenes expanding daily from ongoing satellite missions. Thanks to the powerful computing power and cloud-based data storage features of GEE, research on large-scale environmental monitoring based on the GEE platform has been carried out in recent years. Since this study involves the extraction and analysis of features of the ecological environment and the urbanization of five provinces and one city in East China over nearly 20 years, using traditional local solutions would consume a lot of time and effort in terms of data acquisition and pre-processing. Considering the unique advantages of the GEE platform in terms of arithmetic power and speed, this paper integrated the data in the GEE platform and preprocessed them accordingly, mainly through GEE.

## 3. Results

### 3.1. East China RSEI and Its Changes

Since five-year intervals of land-use products are used in the subsequent analysis, the RSEI is also calculated at a five-year interval. According to the formula of the RSEI, the quantitative inversion of the RSEI in East China from 2000 to 2020 was carried out in this paper with an interval of 5 years. The results are shown in Figure 3. From the calculation results, it can be seen that the RSEI values in East China are high in the south and low in the north. The RSEI values in the economically developed areas such as Jiangsu and Shanghai have been low, the northern part of Anhui shows a lower-magnitude increase, and the RSEI values in most of Fujian Province have been high.

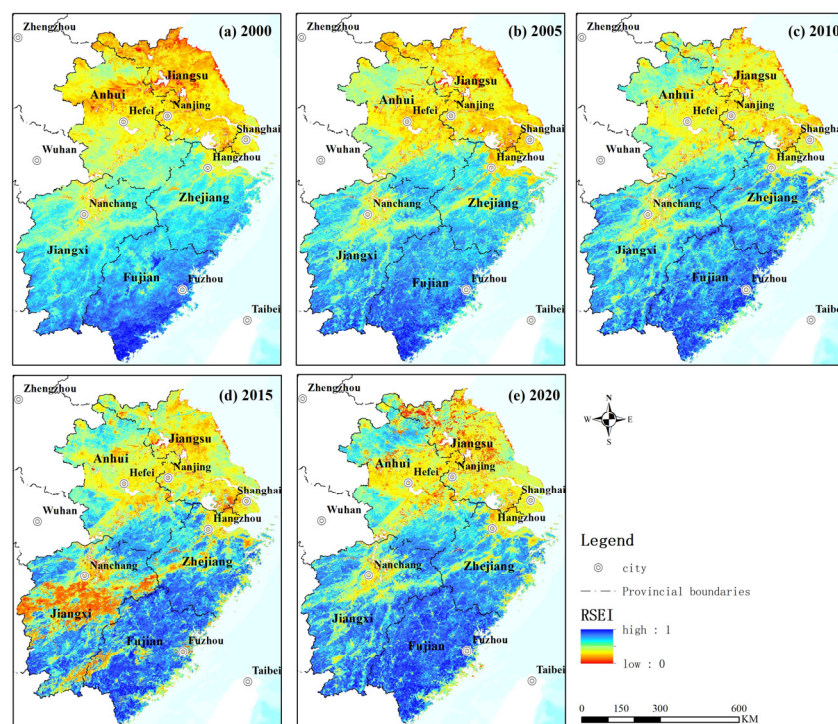


**Figure 3.** The distribution of RSEI values in East China for 2000 (a), 2005 (b), 2010 (c), 2015 (d), and 2020 (e).

Table 1 show the mean RSEI values in East China and its sub-provinces (municipalities directly under the central government). The mean RSEI value in Fujian Province showed a relatively stable increasing trend (19%) during the study period, while Anhui Province and Zhejiang Province showed a small decrease in 2005, followed by a slow increasing trend, and the mean RSEI value in Shanghai and Jiangsu showed a fluctuating characteristic of “decreasing and then increasing”, and a large decrease in the whole monitoring period (32.4%, 25.8%, and 25.8%, respectively).

**Table 1.** Mean RSEI values of provincial units across different years.

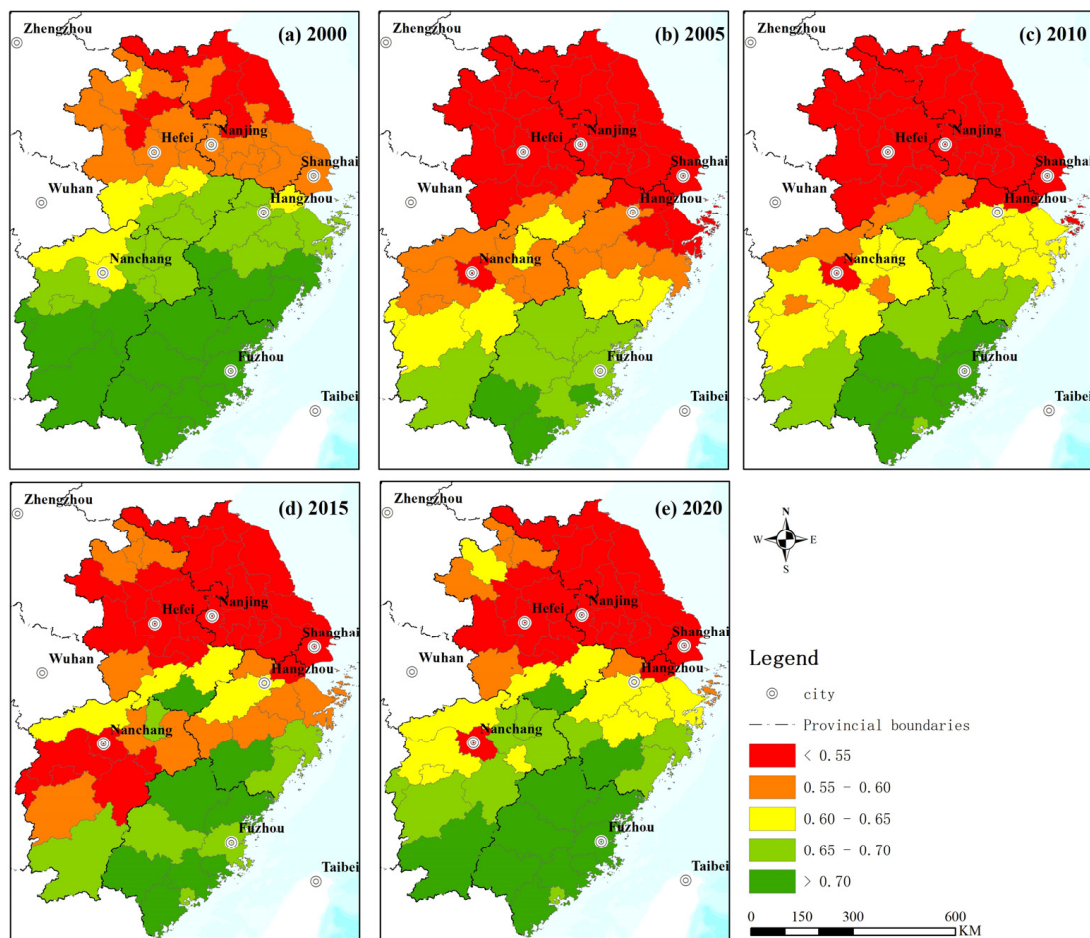
Province	2000	2005	2010	2015	2020
Shanghai	0.78	0.37	0.43	0.42	0.46
Jiangsu	0.71	0.38	0.43	0.45	0.45
Zhejiang	0.70	0.57	0.63	0.63	0.66
Anhui	0.61	0.48	0.51	0.54	0.55
Fujian	0.58	0.70	0.72	0.72	0.78
Jiangxi	0.55	0.61	0.63	0.56	0.68
East China	0.67	0.55	0.59	0.58	0.63

Figure 4 shows the RSEI results for cities in East China in different years, and the natural intermittent occurrence is used for grading. It can be seen that the RSEI values of each city group show obvious spatial heterogeneity in terms of distribution. In 2000, the cities with low mean RSEI values were located in the northern part of the study area, including Anhui, Zhejiang, and Jiangsu provinces. There were seven urban units with low mean RSEI values, located in Anhui and Jiangsu, including Xuzhou, Bengbu, and Huainan. In 2005, the number of cities with low average RSEI values increased to 32, including all cities in Jiangsu Province (13), most cities in Anhui Province (13), 4 cities in the north-central region of Zhejiang Province, Nanchang City in Jiangxi Province, and Shanghai City. The ecological environment of the cities in northern Jiangxi province shows a clear deterioration, with six cities with medium RSEI mean values.

In 2010, the number of low RSEI cities decreased slightly (31) compared with 2005; Hangzhou, Jinhua, Ningbo, and Taizhou in central Zhejiang Province changed from low or lower to medium, and Quzhou, Lishui, and Wenzhou changed from low or medium to higher. The mean RSEI values of Yichun and Shangrao in Jiangxi Province changed from lower to medium. In 2015, the number of low RSEI cities remained high and was basically the same as that in 2010, but the mean RSEI values of Bozhou, Huabei, and Suizhou in Anhui Province increased slightly, changing from low to lower. Pingxiang, Yichun, Xinyu, Fuzhou, and Yingtan in Jiangxi Province changed to the lower class. Quzhou, Jinhua, Ningbo, and Shaoxing in Zhejiang Province changed from medium to lower. In 2020, the number of low RSEI cities remained the same as in 2015, with five lower RSEI cities, mainly in northern and southern Anhui Province, and medium RSEI cities in central Zhejiang Province and northern Jiangxi Province. Fujian Province still maintained a high RSEI values.

According to the changes in the RSEI values between 2000 and 2020, the areas where the RSEI values declined in the past 20 years were mostly located in northern Anhui and southern Jiangsu, while the RSEI values rose in the vast majority of locations, with Zhejiang Province showing an initial decline and then a rise, and northern Zhejiang Province remaining a low-value area. The RSEI value of Fujian Province fluctuated but was maintained at a high level. The relatively obvious changes in Jiangxi province mainly occurred in several cities in the north near Nanchang, where the average RSEI value significantly dropped.

In general, the average RSEI values in East China steadily increased over the past 20 years, and the ecological environment improved, but the regional differences are still significant. The ecological pressure was significantly reduced in the southern part of Anhui Province and the northern part of Jiangxi Province, while the ecological pressure in Zhejiang Province, Jiangsu Province, and Shanghai City is still not ideal.



**Figure 4.** The mean RSEI value distribution of municipal units in different years: (a) 2000; (b) 2005; (c) 2010; (d) 2015; (e) 2020.

### 3.2. Cluster Analysis of RSEI Features

The overall ecological conditions in East China are still spatially heterogeneous, although there is a trend of improvement. According to the local Moran's I diagram (Figure 5), it can be seen that during the decade of 2000–2010, rising RSEI values (ecological improvement) were mainly distributed in southern Zhejiang Province (Quzhou, Shaoxing, and Ningde), Ningde, Fujian Province, and northern Anhui Province (Bozhou and Huabei), and declining RSEI values (ecological deterioration) were mainly located in the central-eastern part of Jiangsu Province, the central part of Anhui Province, Shanghai, and northern Zhejiang Province. During the decade of 2010–2020, the rising RSEI values were mainly located in the northwestern part of Fujian Province, and the declining RSEI values were mainly located in the central-eastern part of Jiangsu Province, the central part of Anhui Province (Hefei and Chuzhou), and Quanzhou City, Fujian Province. During these two decades, the rising RSEI values were mainly located in northwestern Fujian Province. The Chinese government launched a pilot ecological civilization construction evaluation and assessment in Fujian Province to explore the establishment of an ecological civilization construction index system. With the promotion of ecological civilization and the strengthening of environmental protection awareness, the vegetation cover in this region significantly increased. The increase in vegetation cover has driven the rise in RSEI values. On the contrary, the number of areas experiencing declining RSEI values in the past 20 years were mainly located in the central part of Jiangsu and Anhui provinces and in Shanghai. The initial ecological conditions in these areas were better than those in other regions due to their more suitable basic conditions, such as geographical location and topography. However, with rapid economic development and urban expansion, impervious surfaces have occupied more and more ecological land at the urban scale, resulting in poorer ecological quality and ultimately affecting the RSEI values of the area.

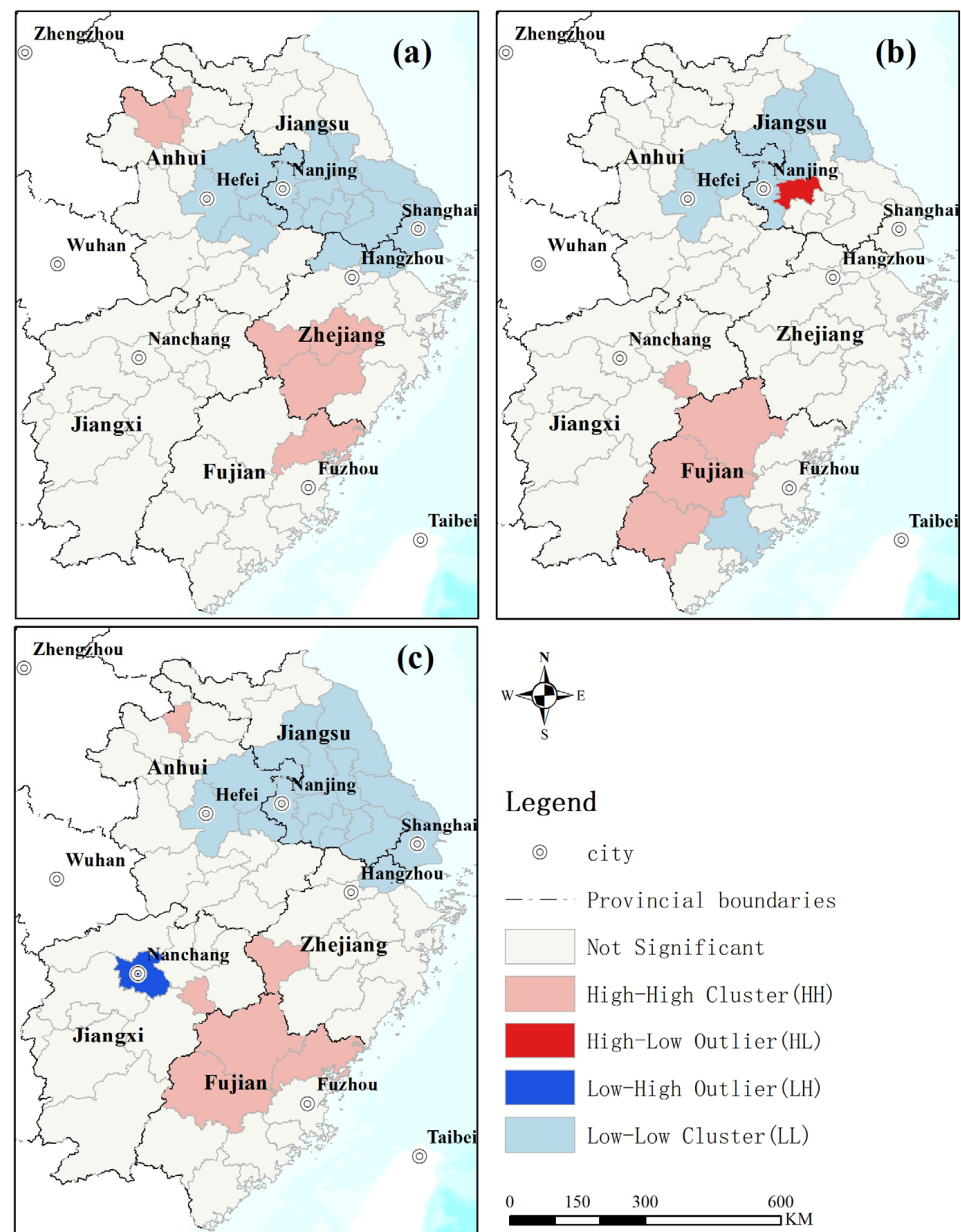


**Figure 5.** The Moran's I map of municipal units in East China for different years: (a) 2000–2010; (b) 2010–2020; (c) 2000–2020.

## 4. Discussion

### 4.1. Characteristics of Land-Use Change

Arable land is the main land-use type in East China, accounting for more than 40% of the regional area (Figure 6). The croplands are mainly located in the northern part of East China in Jiangsu, Anhui, and most of Jiangxi province, and the proportion of croplands is smaller in both southern Zhejiang Province and Fujian Province (Figure 7). Forests and croplands are both major land-use types in East China, and these are mainly distributed in the southern part of the study area, with the highest proportion in Fujian Province, followed by Jiangxi Province and Zhejiang Province, and, to a certain extent, southern Anhui Province. Both wetlands and impervious surfaces accounted for less than 10%, with impervious surfaces mainly being distributed in the densely populated areas in the northern part of the study area and wetlands being more widely distributed. Grasslands have a relatively small distribution of less than 1%, while bare land and permanent snow and ice have a total area of less than 1 km<sup>2</sup>, so these two land-use types were not specifically analyzed.

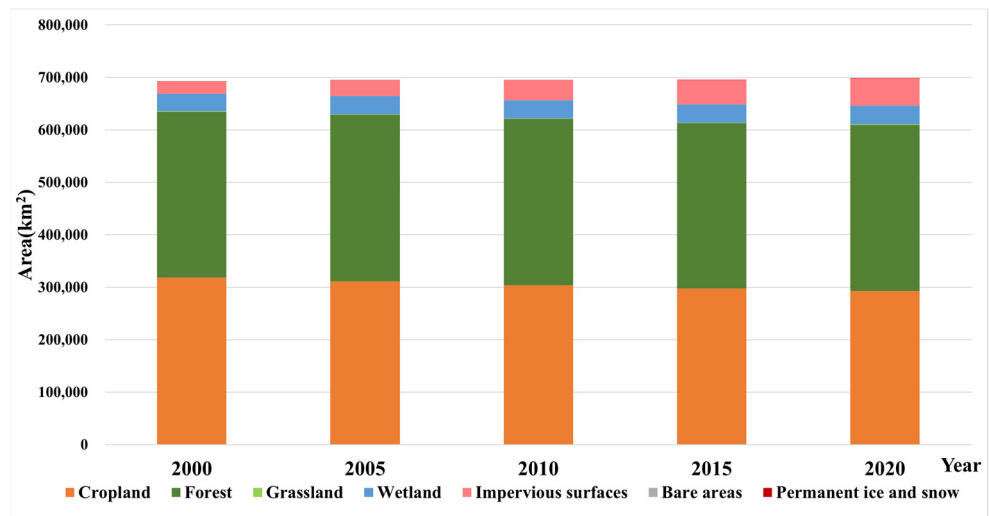


Figure 6. Graph of land-use changes in East China over different years.

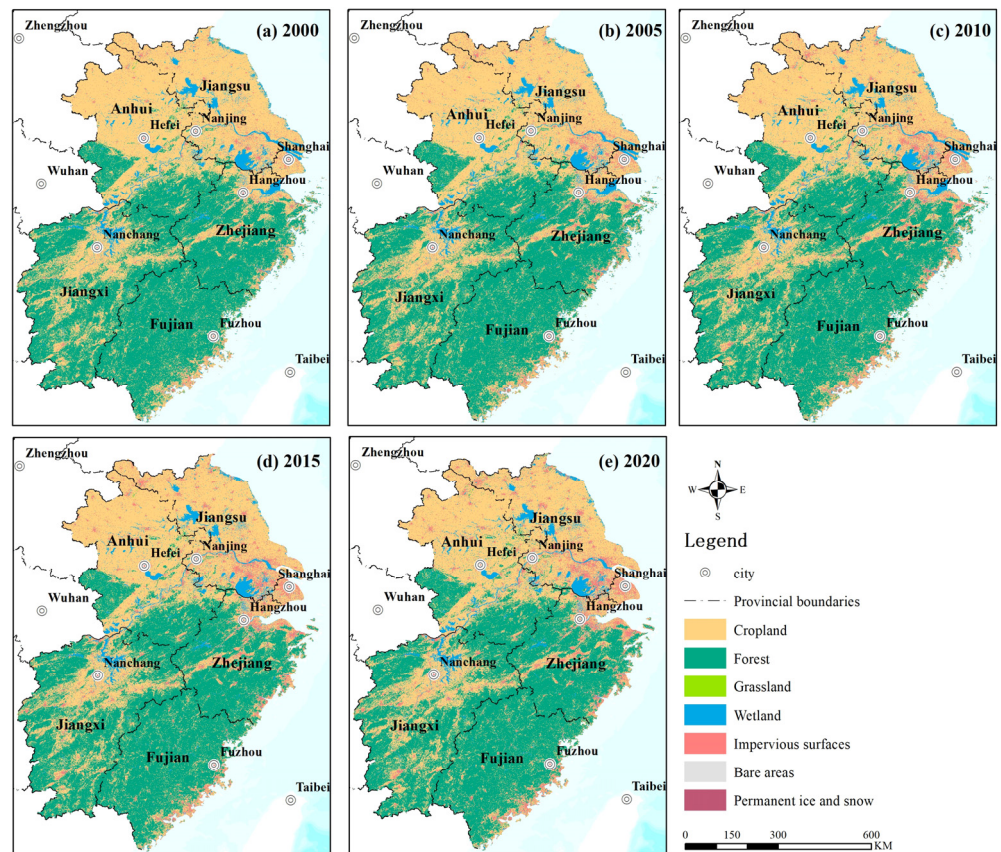
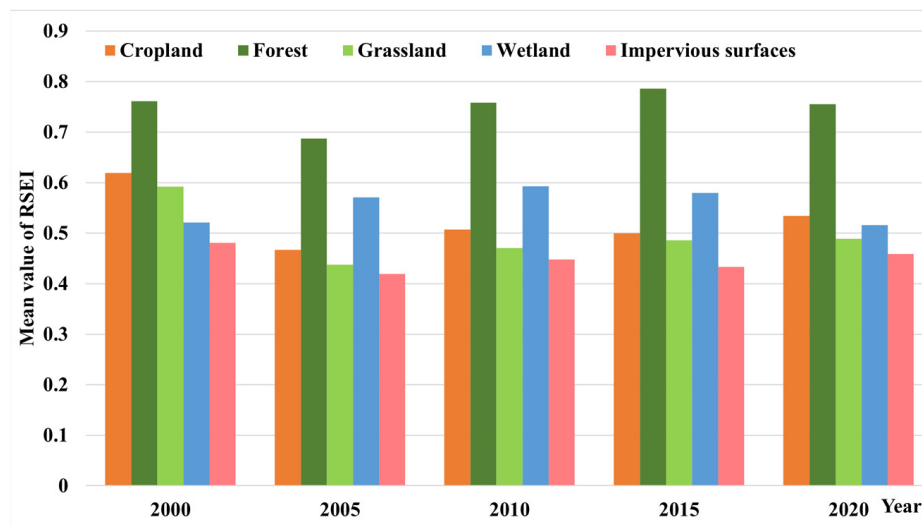


Figure 7. Land-use distribution map of East China from 2000 to 2020: (a) 2000; (b) 2005; (c) 2010; (d) 2015; (e) 2020.

From 2000 to 2020, the land-use changes in East China mainly manifested in an increase in forest land, an increase in impervious surfaces, and a decrease in arable land. The proportion of arable land to total area decreased by about 4.9% over 20 years, while impervious surfaces increased by 4.1%. The increase in impervious surface area was mainly achieved through encroachments on agricultural land.

#### 4.2. Interaction between Land-Use and Eco-Environment

To further investigate the relationship between land use and the RSEI, we counted the mean RESI values of the different land-use types between 2000 and 2020 (Figure 8).



**Figure 8.** Graph of mean RSEI values for different land uses in 2000 to 2020.

The land-use types and RSEI values in different years have good consistency, as shown by the arable land and impervious surfaces tending to have a lower RSEI; on the contrary, wetlands and forests tend to correspond to higher RSEI values, and grasslands have RSEI values in the middle. These indicate that the trend of ecological environmental quality in East China is related to land-use types.

With the development of urbanization, the impervious surface area in Jiangsu and Shanghai has been increasing, which has affected the improvement trend in ecological environment quality to a certain extent, meaning that the RSEI value in the area has shown a decreasing trend. The woodlands in Fujian Province, southern Jiangxi Province and southern Zhejiang Province are the main points of distribution, and the ecological environment in the woodlands in Fujian Province showed an improvement after being damaged [28], so the RSEI value in this area has been increasing. The forest cover of Fujian Province has been increasing and currently stands first in China, so the RSEI values in this region have been increasing [27].

Based on the results of the cluster analysis, a typical city was selected to study the relationship between land-use changes and the RSEI (Figure 9). Due to the different regional land structures, the patterns of changes in RSEI values differ from region to region and can be divided into three patterns: (1) Shanghai and Nanjing are economically developed regions in East China. With rapid economic development, the impervious surface area, mainly construction land, has increased, nearly doubling, and the area of arable land has decreased each year. Impervious surfaces have occupied more and more ecological land, leading to a decrease in vegetation cover, and subsequently causing the RSEI value to decrease. (2) The impervious surface area of Hefei City has increased by nearly 400 km<sup>2</sup>, and the forest area remained basically the same until 2015, so that the RSEI value remained low. The decrease in arable land area in Huabei is mainly caused by the development of urban construction, and mainly concentrated in the time period of 2000–2010, resulting in a poor ecological environment in the region. (3) In Fujian Province, Sanming, Nanping, and Ningde, the main surface-cover type is forest, and the arable land area is small and basically unchanged. Although there was a small increase in impervious surface area, these three cities have a high forest cover, and the overall ecological environment is consistently maintained at a better level.

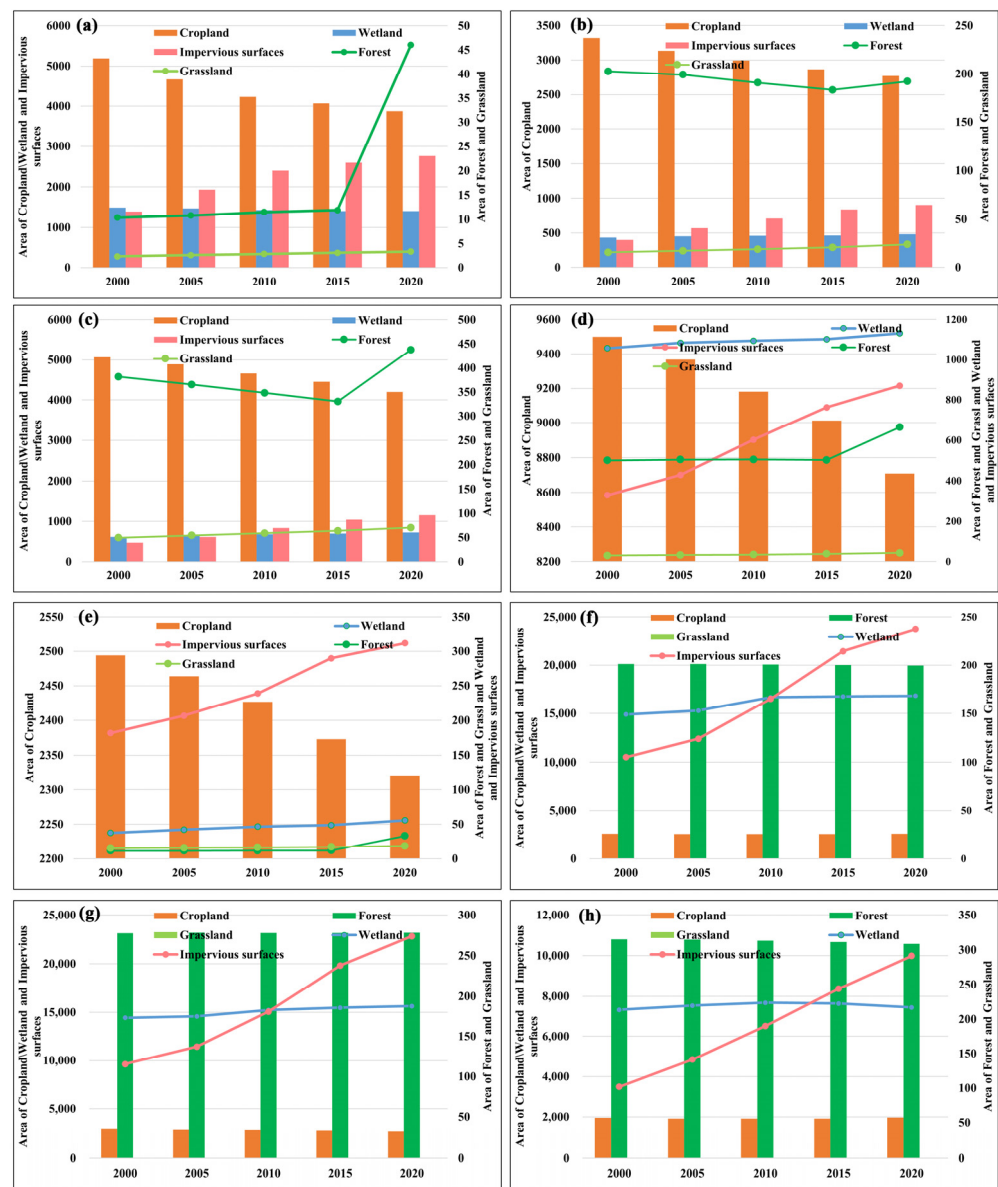


**Figure 9.** Graphs of land-use changes in typical cities from 2000 to 2020. (a–h) land-use change in Shanghai, Changzhou, Nanjing, Hefei, Huaibei, Nanping, Sanming, and Ningde, respectively.

### 4.3. Potential and Limitations

In the past, when using an RSEI to monitor the spatial and temporal changes in regional ecological quality, the monitoring was often constrained by the quality of remote sensing images, and in order to eliminate the influence of image quality, studies mostly selected image data with a better quality and from similar seasons from among annual images, or conducted only small-scale studies [22]. In addition, regions with more clouds often have missing data. The method of substituting neighboring years is usually used [38], which limits the accuracy, comparability, regional scope, and time series length of RSEI studies. In contrast, in this study, the above problems were largely avoided when calculating the RSEI values of Eastern China for the two decades from 2000 to 2020 using the powerful cloud-computing capability provided by GEE. The indicators of greenness, humidity, dryness, and heat in the RSEI were all calculated based on year-round remote sensing data, and the method of extracting the median values by overlaying all images throughout the year enabled us to overcome common problems such as cloud removal and image color differences. The use of GEE can greatly improve the efficiency of image processing and is highly advantageous in research on remote sensing applications over a long period of time and providing a broader prospect for the use of the RSEI.

The existing evaluation index system still needs to be improved. First of all, it is questionable whether the four indicators can comprehensively characterize the regional ecological quality, so the next step could be to increase the number of indicators to improve the representativeness of the indicators for the regional ecological quality. Secondly, when using the GLC\_FCS30 product to analyze its relationship with the RSEI, we reclassified the 29 land-use types included in the GLC\_FCS30 into 7 categories for the convenience of the analysis. For example, "Herbaceous cover" and "Tree or shrub cover" were both defined as cultivated land, which may have had some influence on the accuracy of the results.

## 5. Conclusions

In this paper, based on the Google Earth Engine platform, batch cloud mask removal was used on remote sensing images of East China from 2000 to 2020 to extract remote sensing indexes, such as greenness, humidity, dryness, and heat, to construct an ecological RSEI and evaluate the spatial and temporal changes in regional ecological quality in East China during four different time periods over the past 20 years. The main conclusions are as follows.

- (1) Temporally, the ecological quality in East China over the past three decades shows a trend of first declining and then showing stable growth. Spatially, the ecological quality has obvious spatial heterogeneity, and there is some variability in the mean RSEI value of provincial units, with the RSEI of Fujian Province showing a relatively stable increasing trend during the study period, Anhui Province and Zhejiang Province showing a small decrease in 2005, followed by a slow increasing trend, and the mean RSEI values of Shanghai and Jiangsu Province showing that "The average value of RSEI in Shanghai and Jiangsu has a fluctuating characteristic of falling first and then rising", leading to a large decrease in the whole monitoring cycle.
- (2) During the two decades from 2000 to 2020, the areas with rising RSEI values (ecological improvement) were mainly located in the northwestern part of Fujian Province, and the areas showing declining RSEI values (ecological deterioration) were mainly distributed in the central parts of Jiangsu and Anhui Provinces and in Shanghai. The analysis found a strong correlation between the change in RSEI values and land use. In Fujian and other areas, due to ecological protection measures, the areas of woodland and wetland grew and the RSEI values increased as a result. In some regions, with rapid economic development and urban expansion, impervious surfaces have come to occupy more and more ecological land, leading to a decrease in vegetation cover, which eventually leads to a decrease in RSEI values.

In this paper, by integrating multi-source remote sensing data, and with the help of the GEE cloud platform, we were able to quickly and efficiently achieve a comparative analysis of regional ecological environments and urbanization which can be used for mesoscale development planning. This can provide data support for development planning, ecological monitoring, and environmental protection measures. Compared with previous studies, this solution has the following advantages and potentials.

- (1) It is suitable for medium-scale research applications. Since the introduction of the RSEI, applied analyses based on RSEIs are being enriched. However, the data sources for these RSEI-based ecological condition assessments are mostly focused on higher-resolution satellite imagery represented by the Landsat series, resulting in the study areas being restricted to urban scales. The MODIS data source used in this study has a short revisit period and medium-scale, single-view coverage, which can ensure the consistency and stability of index inversion in medium-scale study areas.
- (2) It is based entirely on remote sensing data sources. Most of the existing studies on the coupled analysis of urbanization and ecological environment use socio-economic statistics as one of the data sources to assess the degree of confounding. On the one hand, complete time series are collected. On the other hand, the differences in statistical quality between regions may also interfere with the accuracy of the analysis results. The unique advantages of remote sensing data in terms of update period and spatial resolution can better meet the requirements of ecological environment monitoring in terms of timeliness.
- (3) There is the potential for the migration of monitoring analysis.

In this paper, the RSEI computation was performed on the CEE platform, which can directly call the massive remote sensing data on the GEE cloud platform for computation and analysis, and greatly reduce the occupation of local computing resources. At the same time, the GEE platform can help overcome the problems of missing remote sensing data, multi-cloud, chromatic aberrations and time inconsistencies, and thus greatly improve the efficiency of image processing and provide

a broader prospect for the application of the RSEI in remote sensing application research with on a large scale and over long periods of time.

**Author Contributions:** Conceptualization, S.W. and X.X.; methodology, S.W. and X.X.; validation, S.W. and M.Z.; formal analysis, S.W. and M.Z.; writing—original draft preparation, S.W.; writing—review and editing, S.W. All authors have read and agreed to the published version of the manuscript.

**Funding:** This research was funded by the National Natural Science Foundation of China, grant number 41901310, and the China Geological Survey, grant number DD20211390.

**Institutional Review Board Statement:** Not applicable.

**Informed Consent Statement:** Not applicable.

**Data Availability Statement:** No new data were created or analyzed in this study. Data sharing is not applicable to this article.

**Acknowledgments:** The authors are grateful for the satellite remote sensing data and open-source data platform and other authors for their help.

**Conflicts of Interest:** The authors declare no conflict of interest.

## References

- Xu, H.Q. A Remote Sensing Urban Ecological Index and Its Application. *Acta Ecol. Sin.* **2013**, *33*, 7853–7862.
- Xiong, Y.; Xu, W.; Lu, N.; Huang, S.; Wu, C.; Wang, L.; Dai, F.; Kou, W. Assessment of Spatial–Temporal Changes of Ecological Environment Quality Based on RSEI and GEE: A Case Study in Erhai Lake Basin, Yunnan Province, China. *Ecol. Indic.* **2021**, *125*, 107518. [[CrossRef](#)]
- Rouse, J.W.; Haas, R.H.; Schell, J.A. *Monitoring the Vernal Advancement and Retrogradation (Green Wave Effect) of Natural Vegetation*; NASA's Goddard Space Flight Center: Greenbelt, MD, USA, 1974; pp. 1–8. Available online: <https://ntrs.nasa.gov/archive/nasa/casi.ntrs.nasa.gov/19730009608.pdf> (accessed on 1 November 2021).
- Fung, T.; Siu, W. Environmental Quality and Its Changes, an Analysis Using NDVI. *Int. J. Remote Sens.* **2000**, *21*, 1011–1024. [[CrossRef](#)]
- Wu, S.-T.; Chen, Y.-S. Examining eco-environmental changes at major recreational sites in Kenting National Park in Taiwan by integrating SPOT satellite images and NDVI. *Tour. Manag.* **2016**, *57*, 23–36. [[CrossRef](#)]
- Li, Y.; Cao, Z.; Long, H.; Liu, Y.; Li, W. Dynamic analysis of ecological environment combined with land cover and NDVI changes and implications for sustainable urban–rural development: The case of Mu Us Sandy Land, China. *J. Clean. Prod.* **2017**, *142*, 697–715. [[CrossRef](#)]
- Wang, Q.; Tenhunen, J.; Dinh, N.Q.; Reichstein, M.; Otieno, D.; Granier, A.; Pilegarrrd, K. Evaluation of seasonal variation of MODIS derived leaf area index at two European deciduous broadleaf forest sites. *Remote Sens. Environ.* **2005**, *96*, 475–484. [[CrossRef](#)]
- Guli-jiapaer, G.; Liang, S.; Yi, Q.; Liu, J. Vegetation dynamics and responses to recent climate change in Xinjiang using leaf area index as an indicator. *Ecol. Indic.* **2015**, *58*, 64–76. [[CrossRef](#)]
- Wang, X.; Zhong, X.; Liu, S.; Liu, J.; Wang, Z.; Li, M. Regional assessment of environmental vulnerability in the Tibetan Plateau: Development and application of a new method. *J. Arid. Environ.* **2008**, *72*, 1929–1939. [[CrossRef](#)]
- Donovan, G.H.; Gatzolis, D.; Jakstis, K.; Comess, S. The natural environment and birth outcomes: Comparing 3D exposure metrics derived from LiDAR to 2D metrics based on the normalized difference vegetation index. *Health Place* **2019**, *57*, 305–312. [[CrossRef](#)]
- Hajjdiab, H.; Ali, S.; Ghazal, M. Novel vegetation estimation index computation in arid environments. In Proceedings of the 2015 IEEE International Symposium on Signal Processing and Information Technology (ISSPIT), Abu Dhabi, United Arab Emirates, 7–10 December 2015; pp. 338–343.
- Monforte, P.; Ragusa, M.A. Temperature Trend Analysis and Investigation on a Case of Variability Climate. *Mathematics* **2022**, *10*, 2202. [[CrossRef](#)]
- Maselli, F. Monitoring forest conditions in a protected Mediterranean coastal area by the analysis of multiyear NDVI data. *Remote Sens. Environ.* **2004**, *89*, 423–433. [[CrossRef](#)]
- Gillespie, T.W.; Ostermann-Kelm, S.; Dong, C.; Willis, K.S.; Okin, G.S.; MacDonald, G.M. Monitoring changes of NDVI in protected areas of southern California. *Ecol. Indic.* **2018**, *88*, 485–494. [[CrossRef](#)]
- Sun, C.; Li, X.; Zhang, W.; Li, X. Evolution of Ecological Security in the Tableland Region of the Chinese Loess Plateau Using a Remote-Sensing-Based Index. *Sustainability* **2020**, *12*, 3489. [[CrossRef](#)]
- Song, H.M.; Xue, L. Dynamic monitoring and analysis of ecological environment in Weinan City, Northwest China based on RSEI model. *Ying Yong Sheng Tai Xue Bao J. Appl. Ecol.* **2016**, *27*, 3913–3919.

17. Hu, X.; Xu, H. A new remote sensing index for assessing the spatial heterogeneity in urban ecological quality: A case from Fuzhou City, China. *Ecol. Indic.* **2018**, *89*, 11–21. [[CrossRef](#)]
18. Yue, H.; Liu, Y.; Li, Y.; Lu, Y. Eco-Environmental Quality Assessment in China's 35 Major Cities Based on Remote Sensing Ecological Index. *IEEE Access* **2019**, *7*, 51295–51311. [[CrossRef](#)]
19. Jing, Y.; Zhang, F.; He, Y.; Kung, H.-T.; Johnson, V.C.; Arikena, M. Assessment of spatial and temporal variation of ecological environment quality in Ebinur Lake Wetland National Nature Reserve, Xinjiang, China. *Ecol. Indic.* **2020**, *110*, 105874. [[CrossRef](#)]
20. Yueriguli, K.; Zibibula, S.; Wang, L. Response of Ecological Environment Change to Urban Construction Land Expansion in Bole City of Xinjiang. *Trans. Chin. Soc. Agric. Eng.* **2019**, *35*, 252–259.
21. Wen, X.; Ming, Y.; Gao, Y.; Hu, X. Dynamic Monitoring and Analysis of Ecological Quality of Pingtan Comprehensive Experimental Zone, a New Type of Sea Island City, Based on RSEI. *Sustainability* **2019**, *12*, 21. [[CrossRef](#)]
22. Zhu, D.; Chen, T.; Zhen, N.; Niu, R. Monitoring the effects of open-pit mining on the eco-environment using a moving window-based remote sensing ecological index. *Environ. Sci. Pollut. Res.* **2020**, *27*, 15716–15728. [[CrossRef](#)]
23. Hansen, M.C.; Potapov, P.V.; Moore, R.; Hancher, M.; Turubanova, S.A.; Tyukavina, A.; Thau, D.; Stehman, S.V.; Goetz, S.J.; Loveland, T.R.; et al. High-Resolution Global Maps of 21st-Century Forest Cover Change. *Science* **2013**, *342*, 850–853. [[CrossRef](#)] [[PubMed](#)]
24. Gorelick, N.; Hancher, M.; Dixon, M.; Ilyushchenko, S.; Thau, D.; Moore, R. Google Earth Engine: Planetary-scale geospatial analysis for everyone. *Remote Sens. Environ.* **2017**, *202*, 18–27. [[CrossRef](#)]
25. Parastatidis, D.; Mitraka, Z.; Chrysoulakis, N.; Abrams, M. Online Global Land Surface Temperature Estimation from Landsat. *Remote Sens.* **2017**, *9*, 1208. [[CrossRef](#)]
26. Kumar, L.; Mutanga, O. Google Earth Engine Applications Since Inception: Usage, Trends, and Potential. *Remote Sens.* **2018**, *10*, 1509. [[CrossRef](#)]
27. Zhang, X.; Wang, W.; Bai, Y.; Ye, Y. How Has China Structured Its Ecological Governance Policy System?—A Case from Fujian Province. *Int. J. Environ. Res. Public Health* **2022**, *19*, 8627. [[CrossRef](#)]
28. Li, S.; Cao, Y.; Liu, J.; Wang, S.; Zhou, W. Assessing Spatiotemporal Dynamics of Land Use and Cover Change and Carbon Storage in China's Ecological Conservation Pilot Zone: A Case Study in Fujian Province. *Remote Sens.* **2022**, *14*, 4111. [[CrossRef](#)]
29. Ma, M.; Wu, H.; Chen, G. Construction of 1:50,000 regional geological map database in East China and its application. *East China Geol.* **2017**, *38*, 228–233.
30. Yang, X.; Hou, Y.; Chen, B. Observed surface warming induced by urbanization in east China. *J. Geophys. Res. Earth Surf.* **2011**, *116*, D14113. [[CrossRef](#)]
31. Zhu, Y.; Wang, H.; Zhou, W.; Ma, J. Recent changes in the summer precipitation pattern in East China and the background circulation. *Clim. Dyn.* **2011**, *36*, 1463–1473. [[CrossRef](#)]
32. Zhang, X.; Liu, L.; Chen, X.; Gao, Y.; Xie, S.; Mi, J. GLC\_FCS30: Global land-cover product with fine classification system at 30 m using time-series Landsat imagery. *Earth Syst. Sci. Data* **2021**, *13*, 2753–2776. [[CrossRef](#)]
33. Liu, L.; Zhang, X.; Gao, Y.; Chen, X.; Shuai, X.; Mi, J. Finer-Resolution Mapping of Global Land Cover: Recent Developments, Consistency Analysis, and Prospects. *J. Remote Sens.* **2021**, *2021*, 5289697. [[CrossRef](#)]
34. Wan, Z. New refinements and validation of the MODIS Land-Surface Temperature/Emissivity products. *Remote Sens. Environ.* **2008**, *112*, 59–74. [[CrossRef](#)]
35. Xu, H.; Wang, Y.; Guan, H.; Shi, T.; Hu, X. Detecting Ecological Changes with a Remote Sensing Based Ecological Index (RSEI) Produced Time Series and Change Vector Analysis. *Remote Sens.* **2019**, *11*, 2345. [[CrossRef](#)]
36. Anselin, L. Local indicators of spatial association—LISA. *Geogr. Anal.* **1995**, *27*, 93–115. [[CrossRef](#)]
37. Zheng, Z.; Wu, Z.; Chen, Y.; Yang, Z.; Marinello, F. Exploration of eco-environment and urbanization changes in coastal zones: A case study in China over the past 20 years. *Ecol. Indic.* **2020**, *119*, 106847. [[CrossRef](#)]
38. Guo, B.; Fang, Y.; Jin, X.; Zhou, Y. Monitoring the effects of land consolidation on the ecological environmental quality based on remote sensing: A case study of Chaohu Lake Basin, China. *Land Use Policy* **2020**, *95*, 104569. [[CrossRef](#)]